An Investigation into the Dissipative Stochastic Mechanics Based Neuron Model under Noisy Input Currents

Humam M. Jassim

Submitted to the
Institute of Graduate Studies and Research
in partial fulfillment of the requirements for the Degree of

Master of Science
in
Computer Engineering

Eastern Mediterranean University
January 2013
Gazimağusa, North Cyprus

Approval of the Institute of Graduate Studies and Research

Prof. Dr. Elvan Yılmaz
Director

I certify that this thesis satisfies the requirements as a thesis for the degree of Master of Science in Computer Engineering.

Assoc. Prof. Dr. Muhammed Salamah
Chair, Department of Computer Engineering

We certify that we have read this thesis and that in our opinion it is fully adequate in scope and quality as a thesis for the degree of Master of Science in Computer Engineering.

Prof. Dr. Marifi Güler
Supervisor

Examining Committee

1. Prof. Dr. Marifi Güler

2. Assoc. Prof. Dr. Işik Aybay

3. Asst. Prof. Dr. Adnan Acan

ABSTRACT

Guided by the existence of a multiple number of gates in each ion channel, it was recently expected that the activity equations of the neuronal dynamics obtain a number of renormalization terms, which play important role in the membranes that are small in size (Güler 2006, 2007, 2008, 2011, 2013). In this thesis, it is attempted to look into the dissipative stochastic mechanics based neuron model under noisy input currents. Specifically, it is concentrated on the role of input noise with reference to the renormalization terms in the model. The investigation shows that the use of noise in the inputs can improve the spiking rates and the spike coherence values, especially in the presence of the renormalization terms.

Keywords: Ion Channel Noise, Stochastic Ion Channels, Neuronal Dynamic, Hindmarsh-Rose Model, Dissipative Stochastic Mechanism Model

ÖZ

Nöron zarlarındaki ion kanallarının çoklu geçit içermesinden dolayı, küçük boyutlu sinir hücresi dinamiğinin renormalizasyon terimleri içermesi gerektiği son yıllarda ileri sürülmüştür (Güler 2006, 2007, 2008, 2011, 2013). Bu tezde, yukarıdaki kapsamda ortaya konulan disipatif stokastik mekanik nöron modeli gürültülü girdi akımları altında incelenmiştir. Renormalizasyon terimlerinin varlığının etkisi özellikle bu kapsamda irdelenmiştir. Ateşleme oranlarının ve uyumluluğunun renormalizasyon ile arttığı gözlenmiştir.

Keywords: İon kanal gürültüsü, Stokastik ion kanalı, Nöron dinamiği, Hindmarsh-Rose modeli, Disipatif stokastik mekanik nöron modeli

I dedicate this thesis to my mother, father, two brothers, sister, uncles, aunties, cousins and to all my friends.

ACKNOWLEDGMENT

I sincerely acknowledge all the help and support that I was given by Prof. Dr. Marifi Güler whose knowledge, guidance, and effort made this research go on and see the light.

My deep gratitude to my mother and father for the support, effort, pain, and patience whom I own the success of my life to them. Special thanks go to my twin brother Hayder and my friends Mohammed Namik, Ahmed Mahmoud, Hossam Nofal, Ahmed Zaid, Saif Anwer, Ahmed Salah, Omar Hayman, Mustafa Ibrahim, Liwaa Hussein, Abdullah Abdul Sattar, Anas Qasim, Ahmed Hani, Mohammed AL_sayed, Sinan Hazem and to all my friends for their help and support.

TABLE OF CONTENTS

LIST OF FIGURES

Chapter 1

INTRODUCTION

Neurons exhibit electrical action which is in nature known to be stochastic (Faisal 2008). The external noise from the synapses is the main cause for stochastic. Still the interior noise, which participates to the gating probabilistic nature of the ion channel, and also it can have important effects on the neuron's dynamic performance as displayed by the experimental studies (Kole 2006; Jacobson et al. 2005; Sakmann and Neher 1995) and by the numerical simulations or theoretical researches (Chow and White 1996; Fox and Lu 1994; Schmid et al. 2001; Schneidman et al. 1998).

Neuronal dynamics under the effect of channel fluctuation is usually modeled with stochastic differential equations acquired by using some vanishing white-noise conditions into the fundamental deterministic equations (Fox and Lu 1994). The dissipative stochastic mechanics (DSM neuron) based neuron model raised by Güler (2006, 2007, 2013), is a special case of this. The DSM model has some forms of functionality named the renormalization terms, as well as some vanishing white-noise conditions in the activity equations. The DSM model has been studied in numerical detail for its time independent input current's dynamics (Güler 2008, 2013); it was established that the corrections of renormalization increases the changes in behavior from quiescence to spiking and from tonic firing to bursting. It was further established

that the existence of renormalization corrections can result in faster temporal synchronization of the electric coupled consecutive discharges of two neuronal units (Jibril and Güler 2009). In this thesis, the DSM model is investigated in the situation of noise fluctuating input currents and concentrates on what role the renormalization terms and noise could have on the spiking rates and the spike coherence values.

Chapter 2

NEURON STRUCTURE

2.1 Morphological and Structural

Neurons are the brain’s most important blocks that are specialized in generating electrical signals due to the impact of chemical and other inputs, and pass them on to other cells. Neuron cells consist of two basic parts: dendrite and axon. Dendrite receives input signals from other neurons and carries them to the neural cell main body called soma. The axon then propagates the output of the neural to other cells. Dendrite structure is like a branch of a tree which increases the surface area of the cell, enhancing the neuron capability to receive inputs from many other neurons through synaptic connection. Figure (1) shows the structure of neurons and information flow. Single neuron's axon can propagate a large proportion of the brain or, in some cases, the whole body.

It was shown that cortical neurons typically send out about 40 mm of axon and 4 mm of dendrite cable in their branches to dendritic trees (Dayan Abbot 2002).

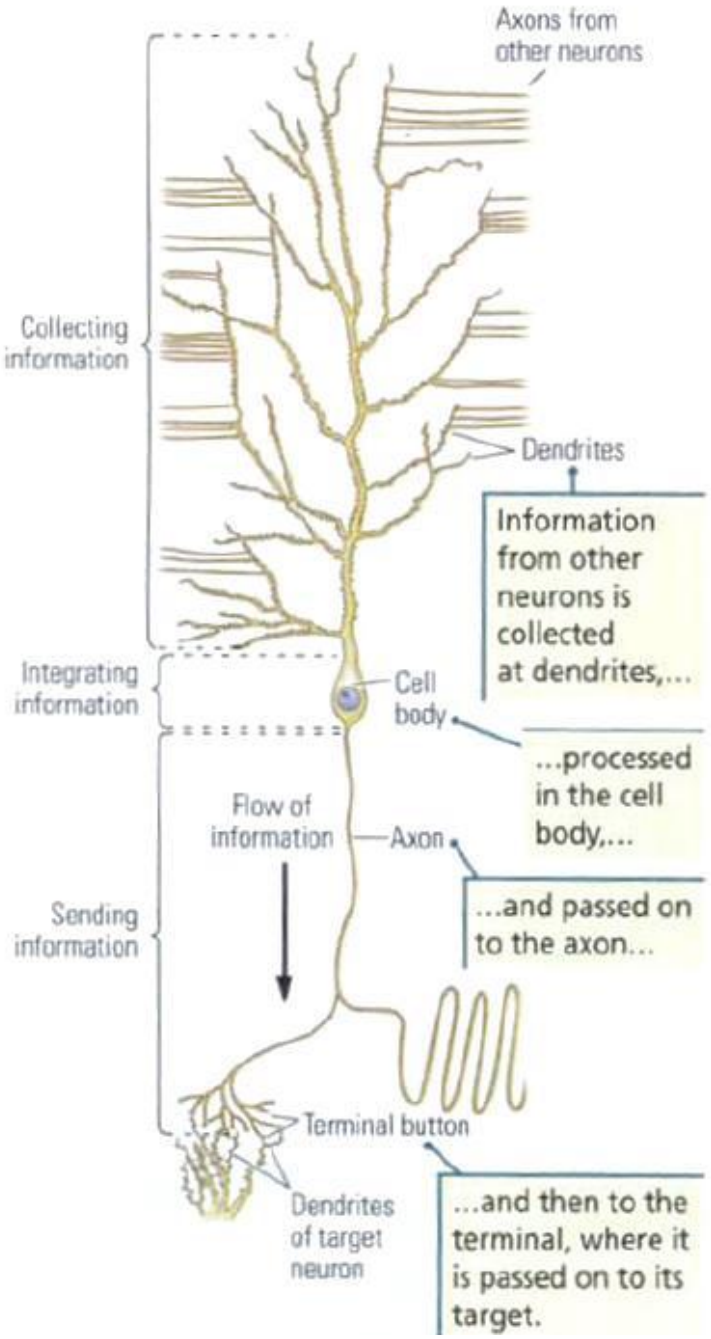

Figure 1: Neuron information flow (Kolb and Whishaw 2009).

2.1.1 Membrane Proteins

Proteins embedded in cell membrane transport substance through it. Knowing how proteins work is necessary to comprehend the tasks of neurons. The protein's job is an emergent property of its form or the capability to change its form .Three classes of membrane proteins can be described that help in passing substance on through the membrane. The three classes of protein are pumps, gates, and channels.

2.1.1.1 Pumps

In some cases, the membrane protein operates as a pump, a transporter molecule that requires energy to move substances across the membrane. For instance, one protein can transfers two kinds of ions by changing its shape to pump Na+ ions in one end and K+ ions in the other end. Many substances are transferred using protein pumps.

2.1.1.2 Gates

Some protein molecules have an important feature which is their capability to change shape. There are gates that function by changing shape when different chemicals bind to them. In these situations, the protein molecule that is embedded works as a lock. When a key matches the size and shape is inserted into the gate and turned, the locking device changes shape and will be activated. Other gates change shape under specific conditions in their environment, such as temperature change or electrical charge.

2.1.1.3 Channels

Some membrane proteins are shaped in such a way that they generate channels or holes, through which substance can move. Various types of proteins with different-size holes allow distinct substances to enter or leave the cell. Protein molecules that serve as

channels are usually calcium (Ca2), sodium (Na+), Potassium (K+), and chloride (Cl-) ions.

Pumps, gates, channels perform significant roles in neuron's capability to transport information.

2.1.2 Synapses

Synapses are shaped in the form of a junction between two consecutive neurons when the axon of afferent neuron is connected to the efferent one and grants a way to carry the information to other cell axon’s end at the synapses. The voltage passing through the action potential opens ion channels creating a stream of Ca2+ that will cause a neurotransmitter to release. Receptors bind the neurotransmitter at the signal receiving or post synaptic side of the synapse leading to the opening of ion-conducting channels. Depending on the ion flow’s nature, the synapses can have inhibitory, depolarizing, or excitatory, typical hyper-polarizing, effects on the post synaptic neuron (Dayan and Abbot 2002).

Synapses are not scattered randomly over the external surface of the dendrite. Generally, inhibitory synapses are proximally more than excitatory synapses, despite the fact that they also present at distal dendritic regions and when present on several spines in combination with an excitatory input (Segev in Bower and Beeman 2003). In many systems (e.g., Cerebellar Purkinje and pyramidal hippocampal cells), an input source given is preferential mapped onto a given region in the dendritic tree (Shepherd 1990),

rather than being randomly scattered over the external surface of the dendrite. Electron micrographic images of synapses in neurons are shown in figure (2).

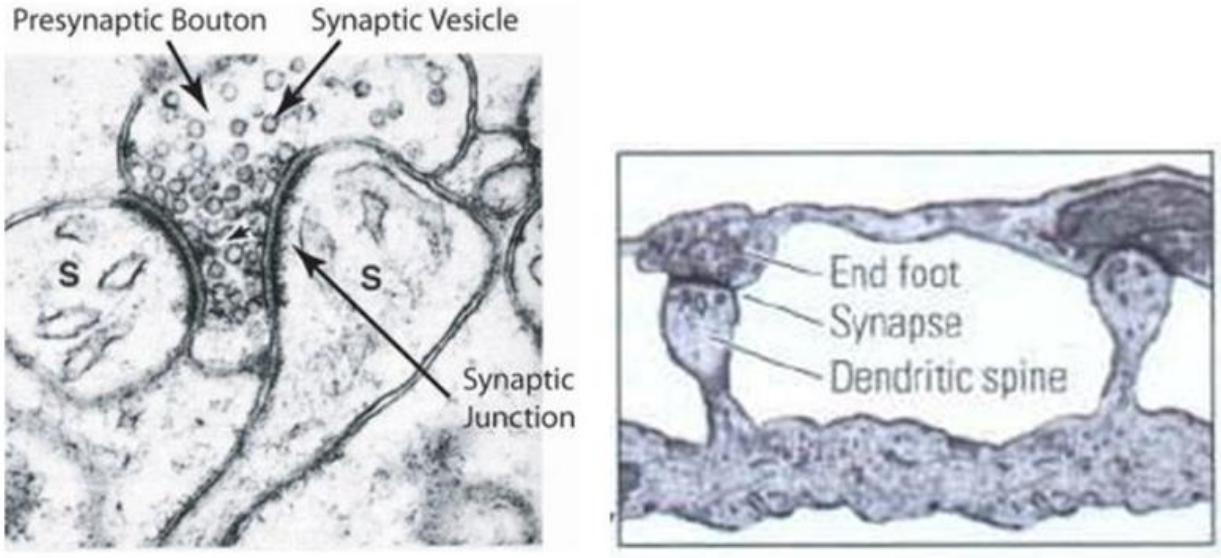

Figure 2: Synapses examples: (A) Electron micrograph of excitatory spiny synapses (s) shaped on the dendrites of a rodent hippocampal pyramidal cell. (B) An electron micrographic figure captured the synapse formed where the terminal bottom of one neuron meets a dendritic spine on a dendrite of another neuron (Kolb and Whishaw 2009).

2.2 Membrane Potential and Neuron Electrical Activity

Membrane potential is known as the difference in electrical potential between the interior and extracellular fluid of the neuron. Under resting situation, the potential of the cell membrane inside a neuron is approximately -70 mV relative to the surrounding area. That voltage, nevertheless, is traditionally assumed to be zero mV for convenience, and the cell state is said to be polarized. This potential is an equilibrium spot at which the ions that flow into the cell equal to those that flow out of the cell. This potential of the membrane difference is sustained by ion pumps located in the cell membrane by keeping concentration on gradients. An example of it, concentration of Na+ in the extracellular of a neuron is much more than inside it, and the K+ concentration in a neuron is significantly higher inside than in the surrounding fluid. As a result, the flow of ions goes in and out of a cell because of voltage and concentration gradients during the cell state of transition.

Current, in the form of positively charged ions flowing out of the cell (or negatively charged ions flowing into the cell) through open channels makes the membrane potential more negative, a process called hyper-polarization. Current streaming inside the cell decreases the negativity of the membrane potential or even makes it positive values. This is known as de-polarization. The membrane potential will rise above a threshold level as a neuron de-polarization is large enough to rise, a process with positive feedback will begin and the neuron creates an action potential, which is nearly 100 mV fluctuation in the electric potential passing through the membrane cell that lasts for about 1ms.

As soon as an action potential occurs, it may be impossible to trigger another spike directly after the earlier one, and this is called the absolute refractory period. The

importance of action potential is that unlike sub-threshold fluctuations that attenuate over distance of at most 1 millimeter they can propagate over large distances without attenuation along axon processes (Dayan and Abbot 2002). Figure (3) explains the neuron voltage dynamic while an action potential which is tuned by a corresponding ion channel activity. In this figure, the resting potential is in its real value of -70 mV.

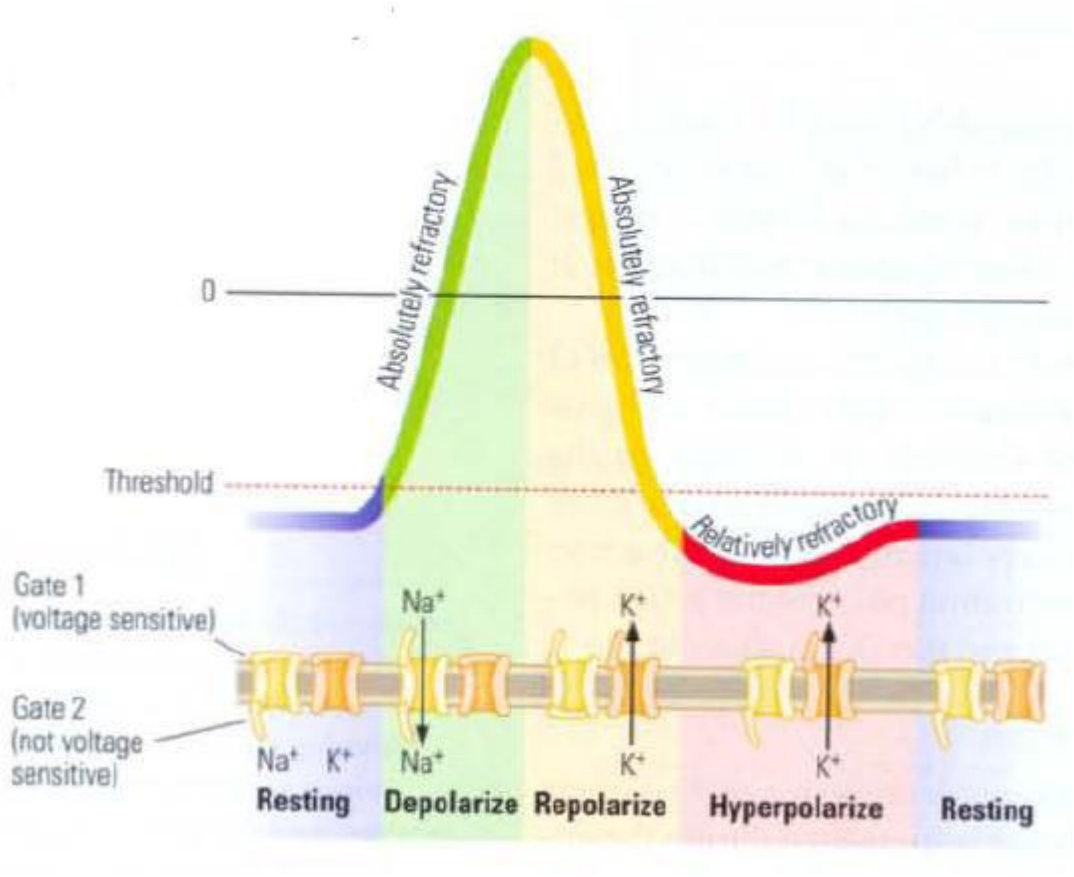

Figure 3: Phases of an action potential initiated by changes in voltage sensitive sodium and potassium channels, an action potential begins with a depolarization (gate 1 of the sodium channel opens and then gate 2 closes). The slower-opening potassium channel contributes on re-polarization and hyper-polarization until the resting membrane potential is restored (Kolb and Whishaw 2009).

Chapter 3

MODELLING THE EXCITABILITY OF NEURON

3.1 Introduction

Over the years, scientists developed many models of neurons for various purposes. These models range from structurally realistic biophysical models, for example, the model of Hodgkin-Huxley (HH), to simpler models, such as the model of Hindmarsh-Rose (HR) that is usually used in studying synchronization theories in the large ensembles of neurons. In different studies, depending on models biological characteristics such as complexity and implementation expenses, various models can be used. However, the methods of modeling neural excitability have been influenced greatly by Hodgkin and Huxley (1952) landmark work (Hodgkin and Huxley 1952).

In this chapter, a brief summary on Hodgkin-Huxley (HH) and Hindmarsh-Rose's (HR) models are presented. Following that, the dissipative stochastic mechanic (DSM) based neuron model will be elaborated that yields the dynamics of Hindmarsh-Rose model in a deterministic condition on which the present study and experiments were conducted.

3.2 The Hodgkin-Huxley Model

Depending on experimental research done on an axon of giant squid using space clamp and voltage clamp techniques, Hodgkin and Huxley (HH) (1952) explained that the current passing through the axon of a squid has only two major ionic elements, I_{Na} and I_k (sodium and potassium channel equivalent elements). The membrane potential V_m has influence on these currents significantly. Accordingly, they developed from their observation a mathematical model to create a model that is still one of the most important model and depending on it, scientists developed lots of realistic neural models (Hodgkin and Huxley 1952).

In this model, section of nerve membrane had an electrical feature that can be sculptured by an equivalent circuit in such a way that current passing through the membrane has two major elements, the first one related with charging the membrane capacitance and the other one related to specific types of ion's movement through membrane. After that, the ionic current is also subdivided into three recognizable currents, sodium I_{Na}, potassium I_K, and small leakage I_L that is mostly conveyed by chloride ions.

The differential equation that corresponds to the electrical circuit is shown below:

$$C_m \frac{dV_m}{dt} + I_{ion} = I_{ext}$$

Where C_m is membrane capacitance, V_m is membrane potential, and I_{ext} is the current that externally applied. I_{ion} is ionic current passing through the membrane and can be calculated from the next equation:

$$I_{ion} = \sum_i I_i$$

$$I_i = g_i(V_m - E_i)$$

I_i here indicates every ionic element that having related conductance g_i and reversal potential E_i.

In the model of a giant squid axon, it has three kinds of currents (I_i): sodium I_{Na}, potassium I_K, and leakage I_L and that will give us this equation:

$$I_{ion} = I_{Na} + I_K + I_L = g_{Na}(V_m - E_{Na}) + g_K(V_m - E_K) + g_L(V_m - E_L)$$

The macroscopic $g_i(g_{Na}, g_K, g_L)$ conductance starts from the united influence of a great amount of membrane microscopic ion channels. Ion channel can be considered as physical gates in a small number that manage the ions flow across the channel. When all the gates in an ion channel are in the permissive condition, ions can flow through the channel, and the channel is open.

3.2.1 The Ionic Conductance

Ions can pass through the channel and it is open when all of the gates for a particular channel are in the permissive state. The formal assumptions used to describe the potassium and sodium conductance empirically achieved by voltage clamp experiments are:

$$g_K = \bar{g}_K n^4$$

$$g_{Na} = \bar{g}_{Na} m^3 h$$

where n, m and h are variable's dynamics of the ion channel gate that will be shown later on, $\bar{g}_i$ is a constant with the scales of conductance per cm^2 (remember that n is between

0 and 1, consequently, the maximum conductance value is needed ($\bar{g}_i$) to normalize the result).

The dynamics of n, m and h are shown below:

$$\dot{n} = \frac{dn}{dt} = \alpha_n(1-n) - \beta_n n \tag{1}$$

$$\dot{m} = \frac{dn}{dt} = \alpha_m(1-m) - \beta_m m$$

$$\dot{h} = \frac{dh}{dt} = \alpha_h(1-h) - \beta_h h$$

where α_x and β_x are rate constants, that fluctuate with voltage but not with time, *n* is a non dimensional variable that can fluctuate between 0 and 1 and shows the individual gate probability of being in the permissive state.

In experiment on voltage clamp, the membrane potential will start rest state at (V_m = 0), and then it is immediately moved to a new voltage clamp $V_m = V_c$. The answer to Eq.s (1) is a simple exponential shown below:

$$x(t) = x_\infty(V_c) - \big(x_\infty(V_c) - x_\infty(0)\big)\exp(-t/\tau_x)$$

$$x_\infty(0) = \alpha_x(0)/\alpha_x(0) + \beta_x(0)$$

$$x_\infty(V_c) = \alpha_x(V_c)/\alpha_x(V_c) + \beta_x(V_c)$$

$$\tau_x(V_c) = [\alpha_x(V_c) + \beta_x(V_c)]^{-1}$$

where x represents time depending gating variables n, m and h .To simplify the formula, $x_\infty(0)$ and $x_\infty(V_c)$ denotes gating variables value at traditional rest state voltage 0 and

clamped voltage V_c . τ_x stands for the constant time course to reach the steady-state value of $x_\infty(V_c)$ when the voltage clamped to V_c .

The constants α_i and β_i are measured in Hodgkin and Huxley as functions of V as follows:

$$\alpha_i = \frac{x_\infty(V)}{\tau_n(V)}$$

$$\beta_i = \frac{1 - x_\infty(V)}{\tau_n(V)}$$

As mentioned before i is a representative index for n, m, and h variables of the ion channel gate. Shown next the rate expressions of constants α_i and β_i that are concluded experimentally:

$$\alpha_n(V) = \frac{0.01(10 - V)}{\exp\left(\frac{10 - V}{10}\right) - 1},$$

$$\beta_n(V) = 0.125 \exp\left(-\frac{V}{80}\right),$$

$$\alpha_m(V) = \frac{0.1(25 - V)}{\exp\left(\frac{10 - V}{10}\right) - 1},$$

$$\beta_m(V) = 4 \exp\left(-\frac{V}{18}\right),$$

$$\alpha_h(V) = 0.07 \exp\left(-\frac{V}{20}\right),$$

$$\beta_h(V) = \frac{1}{\exp\left(\frac{30 - V}{10}\right) + 1}$$

3.3 The Hindmarsh-Rose Model

Despite the fact that Hodgkin-Huxley (HH) can explain neural dynamics of spiking neuron to a certain extent, the complexity of bursting model in HH can be seen in large models. Hodgkin-Huxley studied squid neuron and to be exact in the axon port of it that had Na and K conductance, while in the bursting model of HH there are other conductance kinds, which contribute in a certain role that will make the model slightly more complex.

FitzHugh and Nagumo (FitzHugh R. 1961, Nagumo J. 1962) noticed separately in the Hodgkin-Huxley equations, that in equivalent time-scales the membrane potential V(t) and sodium activation m(t) developed during an action potential, where the change of sodium inactivation h(t) and potassium activation n(t) are similar, even though that's happened in slower time scales. Consequently, now we can represent the simulation spiking response of a model in the following equations:

$$\dot{x} = a(y - f_1(x) + I) \tag{2}$$

$$\dot{y} = b(g_1(x) - y)$$

Where x indicates membrane potential and y denotes the recovery parameter. $f_1(x)$ is represented with cubic function, $g_1(x)$ with linear function, variables a and b are time constants and I(t) is the external current applied or clamping as time function t.

Hindmarsh-Rose benefited from the FitzHugh-Nagumo model to enhance their model, which was a simplified version of the Hodgkin-Huxley equations and substituted the linear function g(x) with a quadratic function so that the model in a long interspaces

interval can accomplish rapid firing. Figure (4) displays the diagram of null-cline of the model of Hindmarsh-Rose in 1982 (Hindmarsh J.L. and Rose R.M 1982).

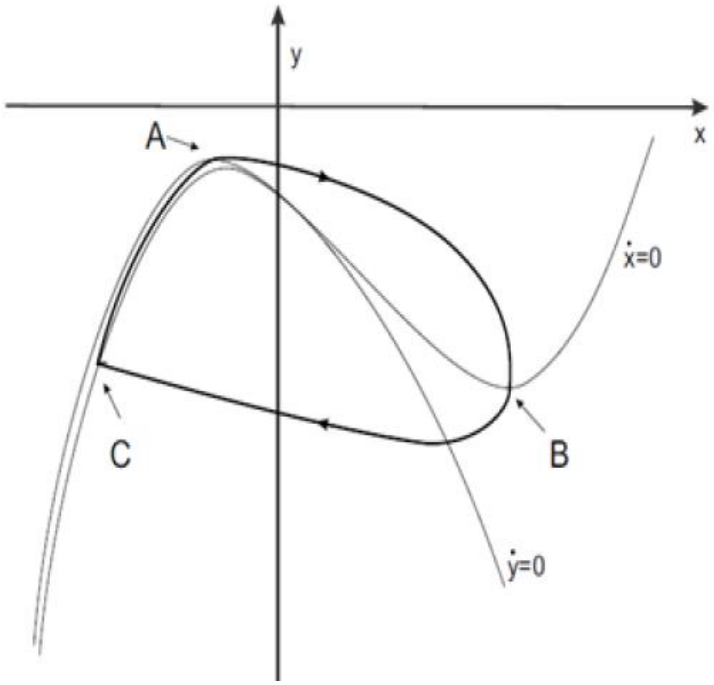

Figure 4: The 1982 HR model phase plane representation. Null-clines $\dot{x}= 0$, $\dot{y}= 0$ (thin lines) and firing limit-cycle (thick line). The model has one equilibrium node (Steur 2006).

The HR model needed more than one equilibrium point to generate burst firing reaction. Basically, the state of Sub-threshold stable resting will have one point and one point inside the cycle of firing limit. To make the null-clines meet and bring additional points of equilibrium, a minor deformation was necessary. The controlling equations were altered to satisfy the requirements as shown in the following equations:

$$\dot{x} = y - f(x) + I$$

$$\dot{y} = g(x) - y$$

where in the simple image of HR model $f(x) = x^3 - 3x^2$ and $g(x) = 1 - 5x^2$. Analysis of the phase plane of the granted equations is shown next page in figure (5).

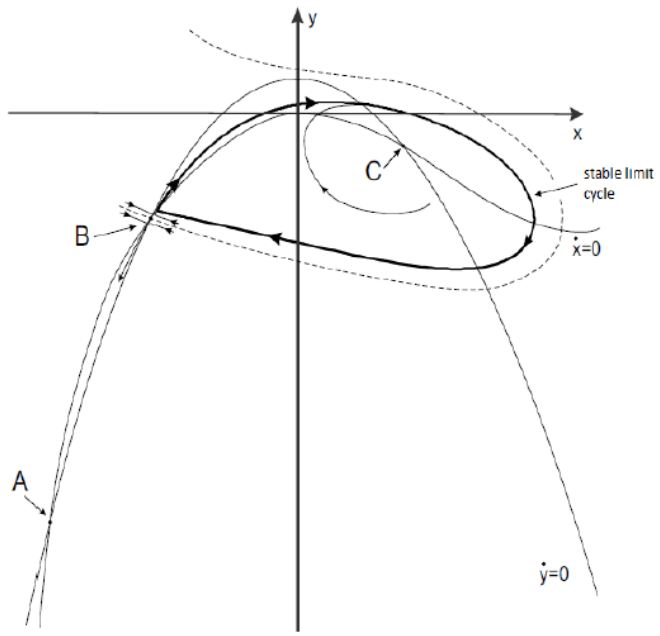

Figure 5: Hindmarsh-Rose model phase plane description. The equilibrium points A, B, and C are a stable node, an unstable saddle, and an unstable spiral, correspondingly, a humble form of f(x) is used in this equation as is indicated $\dot{x} = 0$ null-cline shows (Steur 2006).

The steady point in the figure (5) is the node A that corresponds to the neuron's resting state. By using current pulse de-polarizing that is large enough, $\dot{x} = 0$ null-cline is to be lowered so that the nodes A and B meets and vanishes. Ending firing is impossible by just terminating the stimulus and the state will get out of the limit cycle only after applying a suitable hyper-polarizing pulse. Therefore, to terminate the firing state of the model the term z was inserted. The variable that has been additive stands for a slowly changed current, changing the inserted current I to the effective input I - z. When the neuron is in a firing state, the z value is required to be raised. After this modification, the general set of equations for HR model is as shown below:

$$\dot{x} = -x^3 + 3x^2 + y + I - z \tag{3}$$

$$\dot{y} = 1 - 5x^2 - y$$

$$\dot{z} = r(h(x) - z)$$

It should be noted that the f(x) and g(x) are removed and substituted by their equivalents. Where x indicates membrane potential, y denotes the recovery parameter, and z stands for the current adaptation with time constant r. Parameter z rises up through fire state and goes down through the non-fire state what made the model able to show bursting, chaotic bursting and post-inhibitory rebound are variables h and r. (Hindmarsh and Rose 1984; Steur 2006). Figure (6) in the next page display the analysis of phase plane of the equation (4) applying more complex form of f(x) as suggested in (Hindmarsh and Rose 1984).

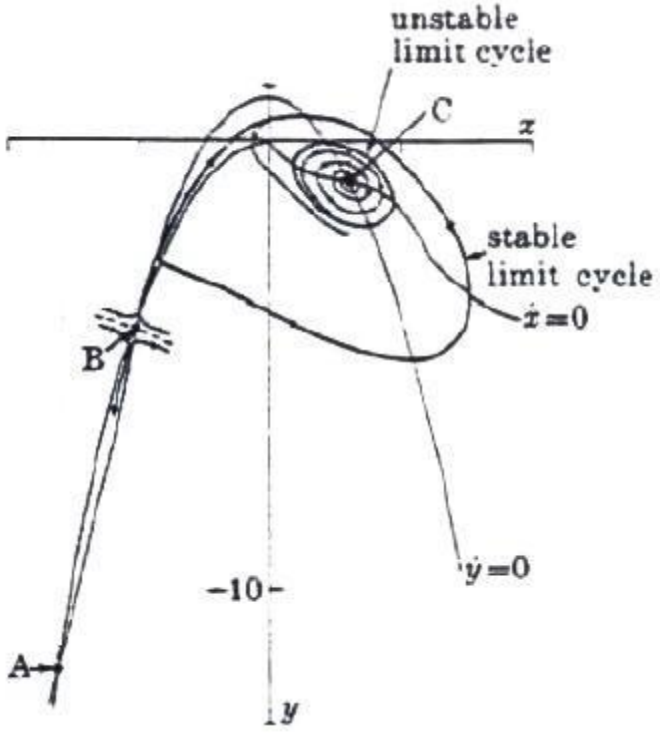

Figure 6: Hindmarsh-Rose model phase plane analysis with the use of more complex form of f(x). The equilibrium nodes A, B, and C are a stable node, an unstable saddle, and an unstable spiral, correspondingly, unstable limit cycle is defined here (Hindmarsh and Rose 1984).

3.4 The Dissipative Stochastic Mechanics (DSM) Neuron Model

The DSM based neuron special formulation comes from a point of view that ion channels conformational fluctuation are subjected to two distinct types of noise. These two noise types were formulated as the intrinsic noise and topological noise. The first one is the intrinsic noise which starts from gating particles voltage dependent movement between inner and outer of the membrane surfaces which is stochastic in nature. Accordingly, gates open and close in a probabilistic manner, this is the average number, not the precise number. Open gates in the membrane are defined by the voltage.

The second one is the topological noise that comes from multiple numbers of gates existences in the channels and contributes to the changes in the open gates topology, instead of the changes in the open gates number.

Curiously, as gating particles during the dynamics do not follow a specific order for the occupation of the available closed gates, and the evacuation of the open gates, the membrane at two distinct times could have an equivalent number of gates being open but two various conductance values. The topological noise is contributed to the suspicion in the open channels numbers that occurs even if open gates numbers are precisely known. Therefore, in defining the dynamics of the voltage, all permits from the gates open topologies which should be well thought of. DSM neuron formula was developed based on Hindmarsh-Rose model (Hindmarsh and Rose 1984) and benefit from the Nelson's stochastic mechanics (Nelson 1966 and 1967), in the dissipation existence, to model the ion channel noise impacts on the membrane voltage dynamics. The topological noise impact on the neuron dynamics gets to be more important in

membranes that are small in size. Accordingly, the DSM neuron functions like the Hindmarsh-Rose model when the membrane size is too large.

The motion equations for both variables cumulants are resulted from the formalism of the DSM neuron. The second cumulants that depict the neuron's diffusive manners do not concern us in this thesis. The first cumulants develop in harmony with the dynamics below:

$$m\dot{X} = \Pi + S_5 I$$

$$\dot{\Pi} = -\left(\frac{3\mathfrak{a}}{\mathrm{m}}\mathrm{X}^2 - \frac{2\mathrm{b}}{\mathrm{m}}\mathrm{X} + \mathrm{S}_0\right)(\Pi + \mathrm{S}_5\mathrm{I}) - \mathrm{S}_1\mathfrak{a}\mathrm{X}^3 + \mathrm{S}_2\mathrm{X}^2 + \mathrm{S}_6\mathrm{X} - \mathrm{S}_3\mathrm{X}_{\mathrm{eq}}(\mathrm{I}) + \mathrm{S}_1\mathrm{I} + \mathrm{S}_7 - (1-\mathrm{r})[\mathrm{k}\left(1 - \frac{\varepsilon_{\mathrm{m}}^{\mathrm{y}}}{\mathrm{m}}\right)\mathrm{z} + (1-\mathrm{k})\left(1 - \frac{\varepsilon_{\mathrm{m}}^{\mathrm{z}}}{\mathrm{m}}\right)\mathrm{y}$$

$$\dot{y} = -y - dX^2 + c + n^y \tag{3}$$

$$\dot{z} = -rz + rh(X - x_s) + n^z \tag{4}$$

$$\Pi(t_0) = y(t_0) - z(t_0) - \mathfrak{a}\left(\mathrm{X}(t_0)\right)^3 + \mathrm{b}\left(\mathrm{X}(t_0)\right)^2 + (1 - \mathrm{S}_5)\mathrm{I}(t_0) \tag{5}$$

where *X* indicates the membrane voltage value expected, and Π matches to the expected value of a momentum-like operator. The additional variables *y* and *z* describe the fast and the slower ion dynamics, respectively. *I* stands for the exterior current inserted into the neuron, and *m* represents the capacitance of the membrane. The variables *a*, *b*, *c*, *d*, *r*, and *h* are constants. *k* is a mixing coefficient presented by *k = 1/(1+r)*. S_i are constants as shown next:

$$S_0 \coloneqq k + (1-k)r$$

$$S_1 \coloneqq S_0 - [k\frac{\varepsilon_m^y}{m} + (1-k)r\frac{\varepsilon_m^z}{m}]$$

$$S_2 \coloneqq k\left(1-\frac{\varepsilon_m^y}{m}\right)(b-d)+(1-k)\left(1-\frac{\varepsilon_m^z}{m}\right)(rb-d)$$

$$S_3 \coloneqq k\varepsilon_u^y+(1-k)\varepsilon_u^z$$

$$S_4 \coloneqq k\frac{\varepsilon_m^y}{m}+(1-k)\frac{\varepsilon_m^z}{m}$$

$$S_5 \coloneqq 1-S_4$$

$$S_6 \coloneqq S_3-S_5 rh$$

$$S_7 \coloneqq (rhx_s+c)S_5$$

Eq. (5) defines Π value at the beginning time t_0 in terms of the beginning values of the other dynamical parameters *X*, *y* and *z*, and the current *I*. *Xeq(I)* bows to the equation:

$$\mathfrak{a}X_{eq}^3-(b-d)X_{eq}^2+h\left(X_{eq}-x_s\right)-c-I=0$$

where x_s is a constant. n^y and n^z in Eqs. (3) and (4) are noises from the Gaussian white kinds with zero means and mean squares presented by:

$$< n^y(t)n^y(t^{'}) >= 2mT\delta(t-t^{'})$$

and

$$< n^z(t)n^z(t^{'}) >= 2rmT\delta(t-t^{'})$$

are obtained by the fluctuation-dissipation classical theorem. T indicates a temperature-like value. The renormalization terms are the conditions with the correction coefficients $\mathcal{E}_m^y$,$\mathcal{E}_u^y$, $\mathcal{E}_m^z$ and $\mathcal{E}_u^z$ that occur in the equations above.

When the noise parameters n^y and n^z are neglected and setting all the correction coefficients to zero, the dynamics of the DSM works in the same way like the dynamics of Hindmarsh-Rose. All the model parameters, even time, are in dimensionless units. The original voltage time series of the membrane for Hindmarsh-Rose's original model

is shown in the Figure (7) for some different constant current inputs. Hindmarsh-Rose model dynamical states are quiescence, bursting (rhythmic with a periodicity in high degree, or chaotic), and tonic firing.

It was shown that the representation of intrinsic noise will get to be more important in small size membranes and it's the same in case of fewer channels in DSM Neuron (Güler 2008). The intrinsic noise can be the source of spiking activity in quiet deterministic model and in large input current values bursting can be caused. In figure (8) the DSM Neuron dynamics in a small size membrane is demonstrated. Notice that renormalization corrections are equal to zero so that the result is studied regardless of the topological noise influence.

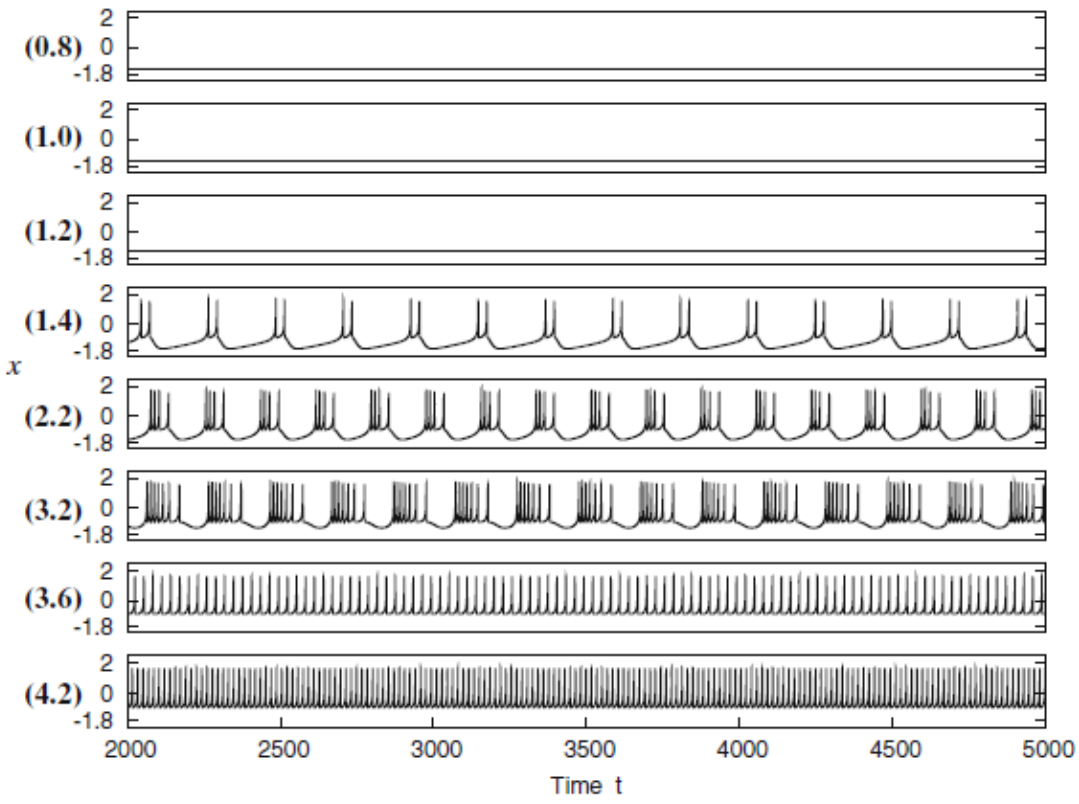

Figure 7: Membrane voltage time series of the deterministic Hindmarsh-Rose model applying the parameter values m = 1, a = 1, b = 3, c = 1, d = 5, h = 4, r = 0.004 and x_s=-1.6; for different constant inputs current values *I*, indicated in a parenthesis on the left of each plot (Güler 2008).

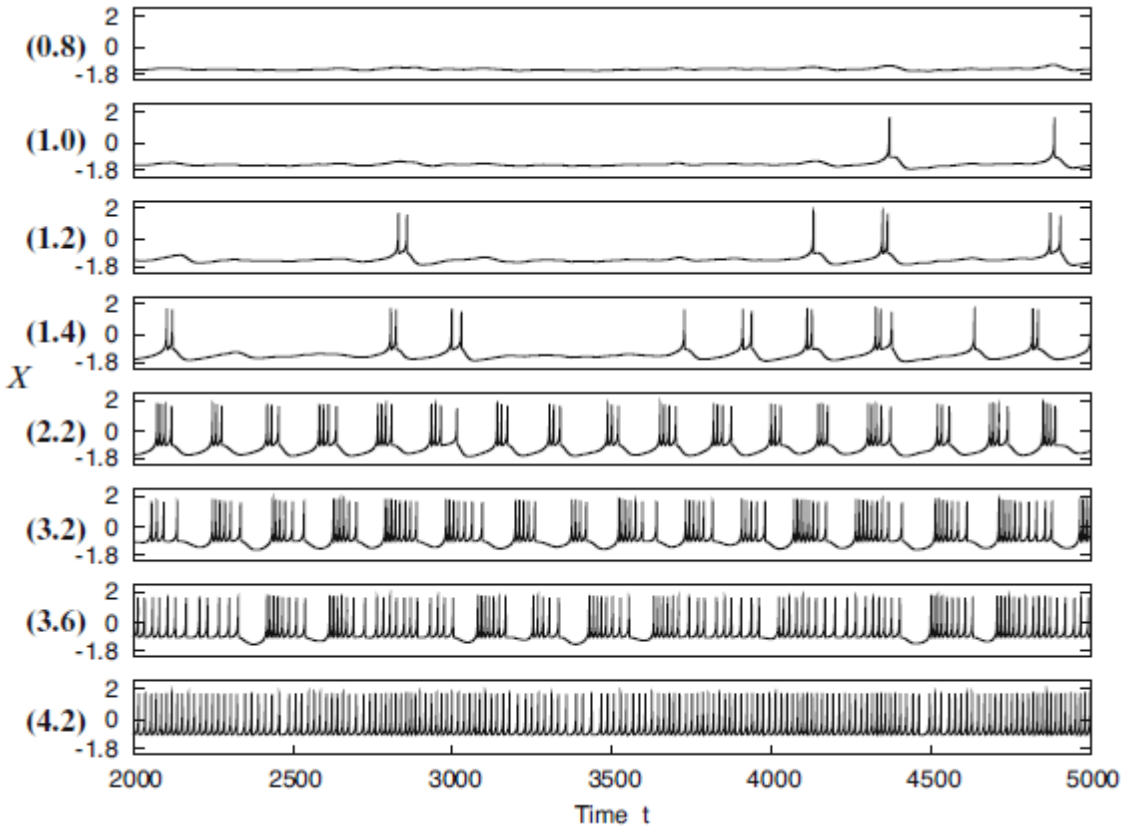

Figure 8: Time series of X when the DSM neuron is exposed just to the intrinsic noise applying the Hindmarsh-Rose $m = 0.25$, $a = 0.25$, $b = 0.75$, $c = 0.25$, $d = 1.25$, $h = 1$, $r = 0.004$ and x_s=-1.6 with the temperature $T = 0.008$. Schemes for different constant inputs current values $4I$ (scaled by the factor of four) (Güler 2008).

Renormalization corrections are caused by the interaction between the topological and intrinsic noises. The existence of correction's parameters further increases the shift in behavior from quiescence to spiking and from tonic firing to bursting to a significant degree and with evidence to this, it causes the bursting activity to occur in a wider domain of input currents. Hence, in the existence of the correction terms, the spiking activity begins to occur at smaller input current values and the bursting activity is extended for higher input current values. The DSM neuron manner under the effect of corrections is displayed next page in figure (9).

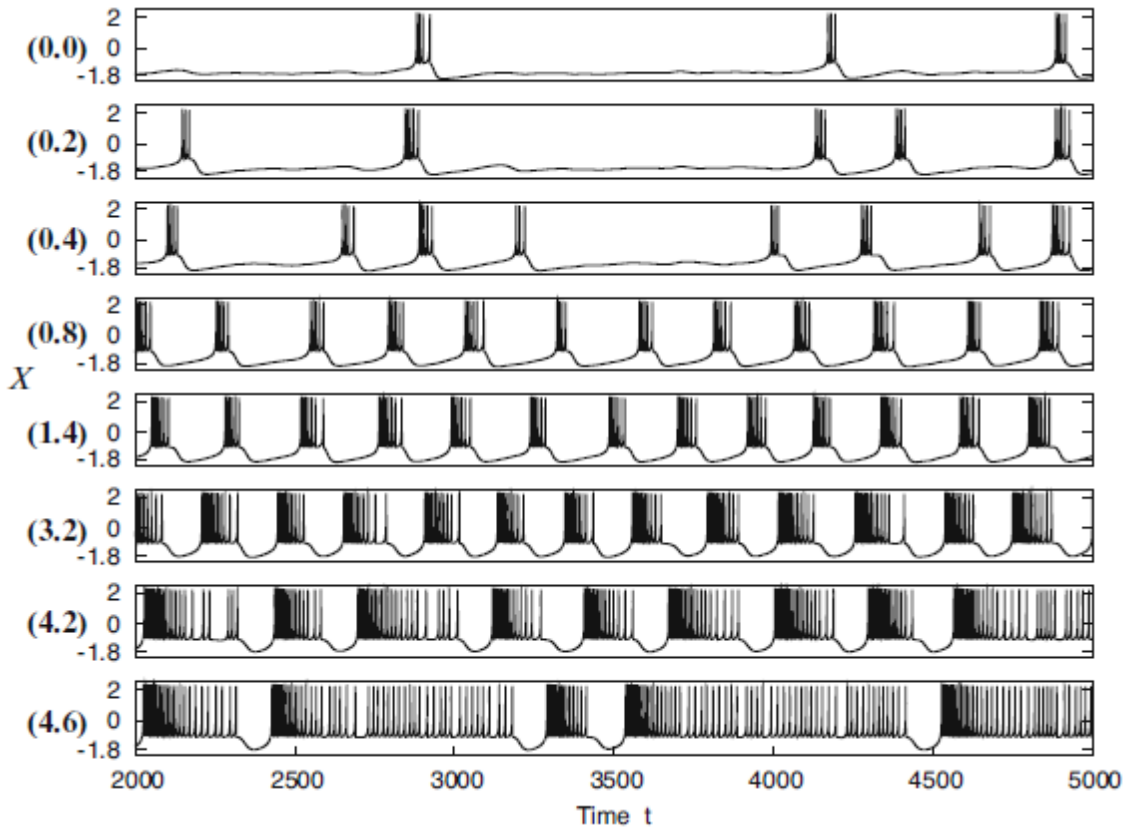

Figure 9: Time series of X using the correction coefficients $\varepsilon_m^y = 0.1$, $\varepsilon_u^y = 1.0$, $\varepsilon_m^z = 0.001$ and $\varepsilon_u^z = 0.005$ with the temperature T = 0.008. The Hindmarsh-Rose parameter are m = 1, a = 1, b = 3, c = 1, d = 5, h = 4, r = 0.004 and x_s=-1.6 (Güler 2008).

3.4.1 Noise in neuronal information processing

Noise can enhance neuronal systems from signal transmission properties point of view under certain conditions. Sub-threshold oscillations in a neuron may have an important effect on the data coding in neurons when magnified by noise (Braun 1998). The perfect noise amount existence in the neuron system may have association with the input signal to enhance signal observation (Gerstner and Kistler 2002).

There are two types of noise; the internal and external which have been explained within the DSM neuron approach model in the third chapter. In this study the noise is a white

Gaussian noise and considered to be one variable containing both the internal and the external noise.

Gaussian noise is statistical noise that has its probability density function equal to that of the normal distribution, which is also known as the Gaussian distribution. In other words, the values that the noise can take on are Gaussian-distributed. A special case is white Gaussian noise, in which the values at any pairs of times are statistically independent (and uncorrelated). In applications, Gaussian noise is most commonly used as additive white noise to yield additive white Gaussian noise.

Chapter 4

NUMERICAL EXPERIMENTS

4.1 The Role Played by the Renormalization Terms and Noise in Computing Spiking Rate and Coherence

Rather than investigating the role of the correction coefficients separately, we take the standard values of epsilons (renormalization terms) as follows ($Y\_m = 0.1$,$Y\_u = 0.5$, $Z\_m = 0.001$, and $Z\_u = 0.005$) and scale them to zero to have a benchmark of various sets of correction coefficients. We use the following periodic input current for the neuron:

$$I = I_{base} + gwn$$

where I_{base} indicates the current and gwn are Gaussian white noise.

The model's behavior is studied in the context of spiking rate and coherence, within the following ranges of the parameters: the time will be measured *mS*, voltage will be measured in *mV*. We used noise variances values between 0 and 2 and will be measured in $\mu A/cm^2$ and I_{base} values between 0.8 and 2.2 and will be measured in $\mu A/cm^2$. The spiking rate when the I_{base} values under 0.8 is small and after the I_{base} pass the values of 2.5 it become too large so in both cases we didn't use that results in this thesis for comparison. Only the optimum result was taken in case of the lowest and highest spiking rate.

In the first set of experiments, the epsilon values and noise were set to zero and by changing I_{base} we obtained the results that are outlined in figure (10). After that, the epsilon values were set to the default values which are ($\varepsilon_m^y = 0.1$, $\varepsilon_u^y = 1.0$, $\varepsilon_m^z = 0.001$ and $\varepsilon_u^z = 0.005$. The noise was not change and remained zero. The experiments were performed by changing I_{base} and the results are obtained and presented in figure (11).

In the second set of experiments, the noise was changed to (0.8). As in previous experiments the renormalization terms were assigned value zero as in the first set of experiments, and when I_{base} value is changed, the results were as in figure (12). Then the default values of the epsilon values were used, the noise was fixed to the same value (0.8) and when I_{base} is changed until it reaches the last value. The results are shown in the figure (13).

The difference of both sets in which the existence and the absence of epsilon value is shown in the figures (14, 15, 16 and 17).

The effect of the renormalization terms appear in significant manner when the value of the I_{base} are below 0.5 and after I_{base} exceed this value the renormalization terms effect will be reduce dramatically and the noise will have the most effect on the neuron behavior as shown in figures (18, 19, 20 and 21).

4.2 Technologies used in this thesis

The DSM neuron model has been developed by Prof. Marifi Güler and some parts have been changed like the main equation in the models in order to make it possible to do the experiments of this thesis. The model has been written by the C++ language. The GnuPlot program was used to plot the results and voltage time series.

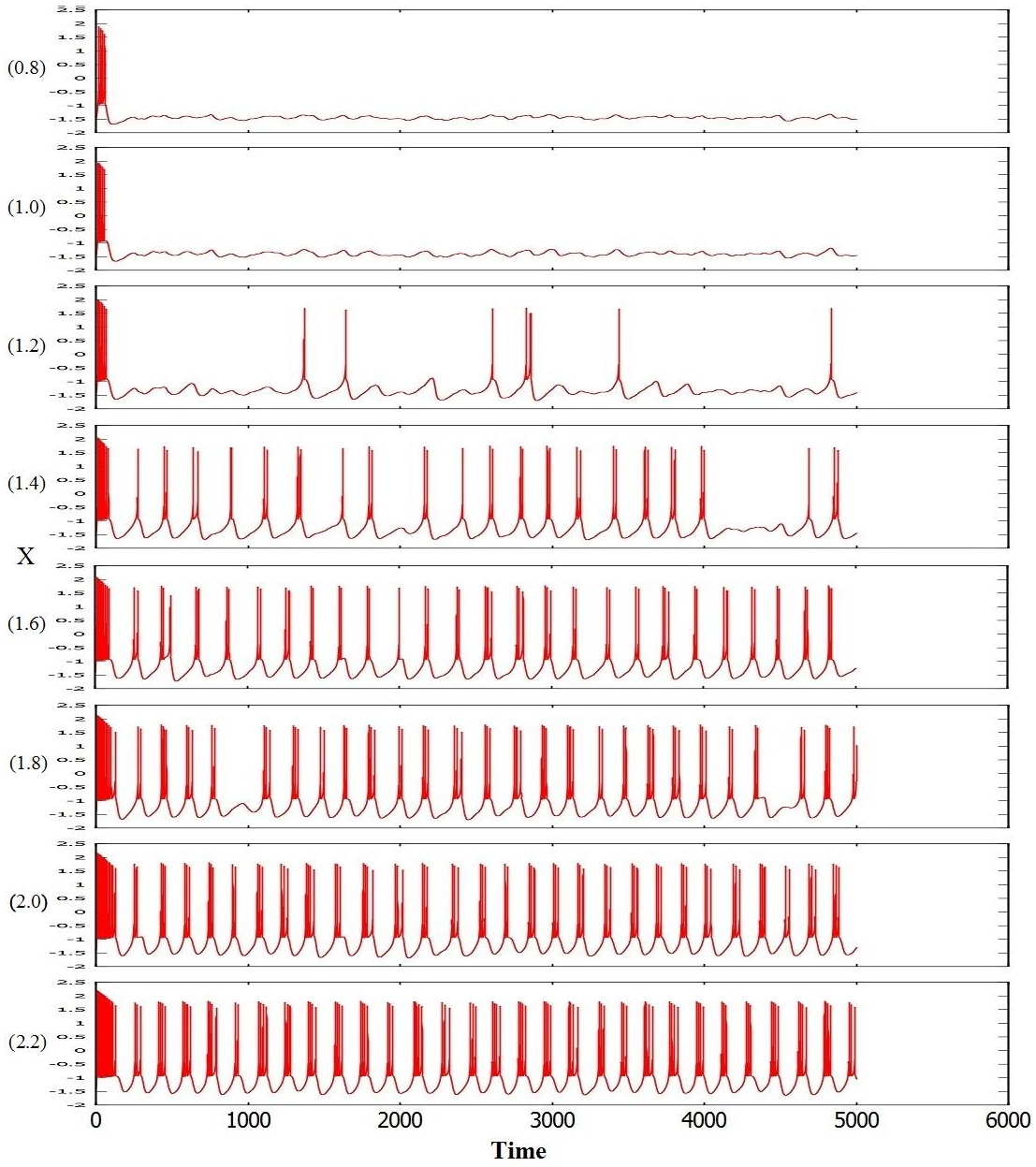

Figure 10: Voltage time series of the membrane deterministic using DSM model for the parameter values m=1, a=1, b=3, c=1, d=5, $x_s = -1.6$, *r=0.004, h=4, T=0.04* and the epsilon values and noise variances are set to be zero using various constant input current values as shown between the parentheses in the lift side of the figure.

In the figure (10) above the experiment was done by fixing the renormalization terms values and the noise variance values to zero. And by changing the I_{base} we get the result shown in the figure above. When the value of I_{base} is small there is no spiking action

and after increasing the value of I_{base} the neuron spiking rate start to increase in a rapid manner and the experiments have a low coherence.

In the figure (11) next, the result is gotten by fixing the renormalization terms values to ($\varepsilon_m^y = 0.1$,$\varepsilon_u^y = 1.0$,$\varepsilon_m^z = 0.001$ and $\varepsilon_u^z = 0.005$) and the noise variance values to zero and when changing the I_{base} the number of spikes in the experiments will increase in slow manner instead of the fast increasing as in the experiments shown in the figure (10) and the coherence will be high in this experiments contrary to the experiments in the figure (10).

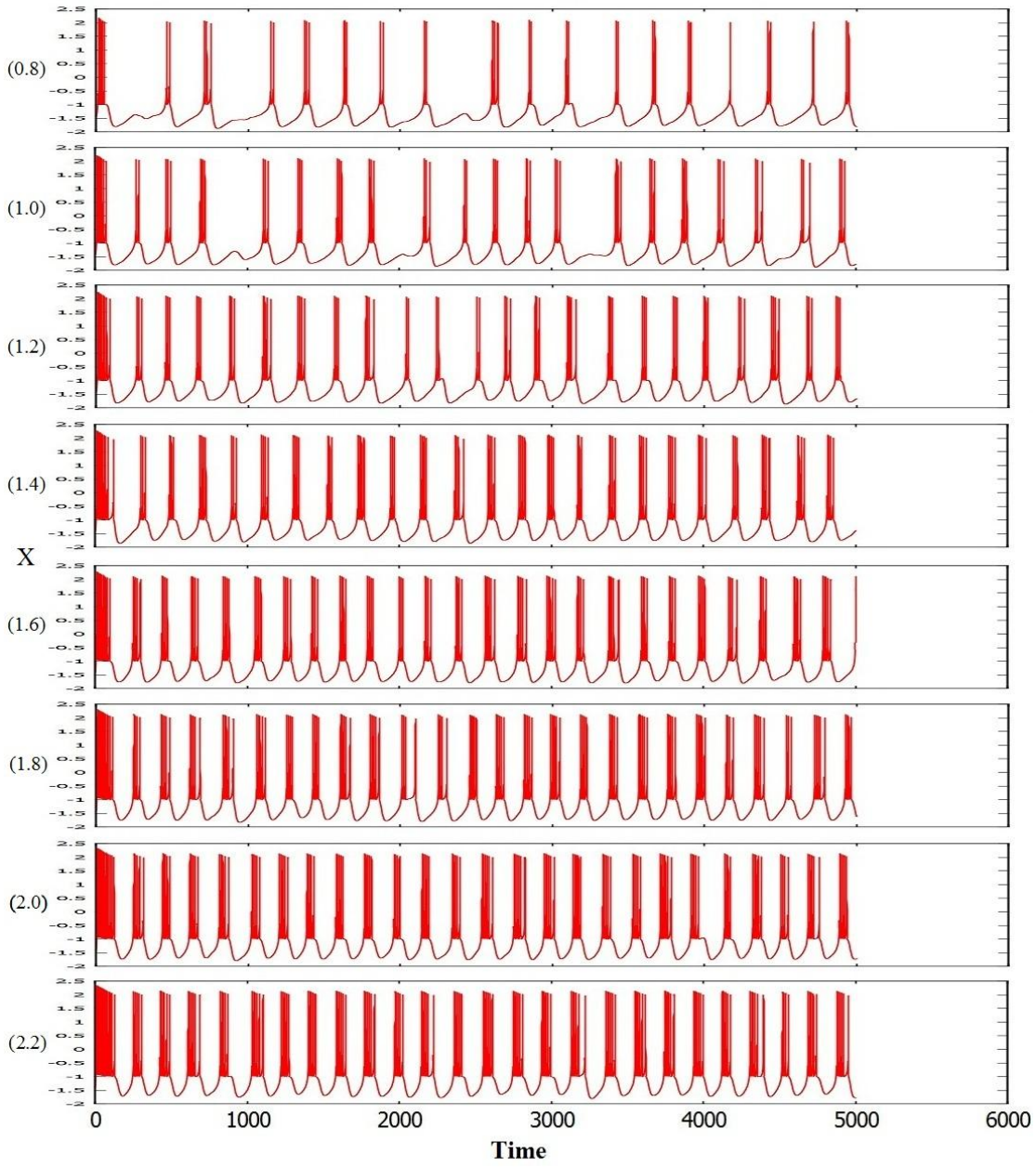

Figure 11: Voltage time series of the membrane deterministic using DSM model for the parameter values m=1, a=1, b=3, c=1, d=5, $x_s = -1.6$, *r=0.004, h=4, T=0.01* and the epsilon values are $\varepsilon_m^y = 0.1$, $\varepsilon_u^y = 1.0$, $\varepsilon_m^z = 0.001$ and $\varepsilon_u^z = 0.005$ using various constant input current values as shown between the parentheses in the lift side of the figure, and the noise variances is set to zero in all the experiments.

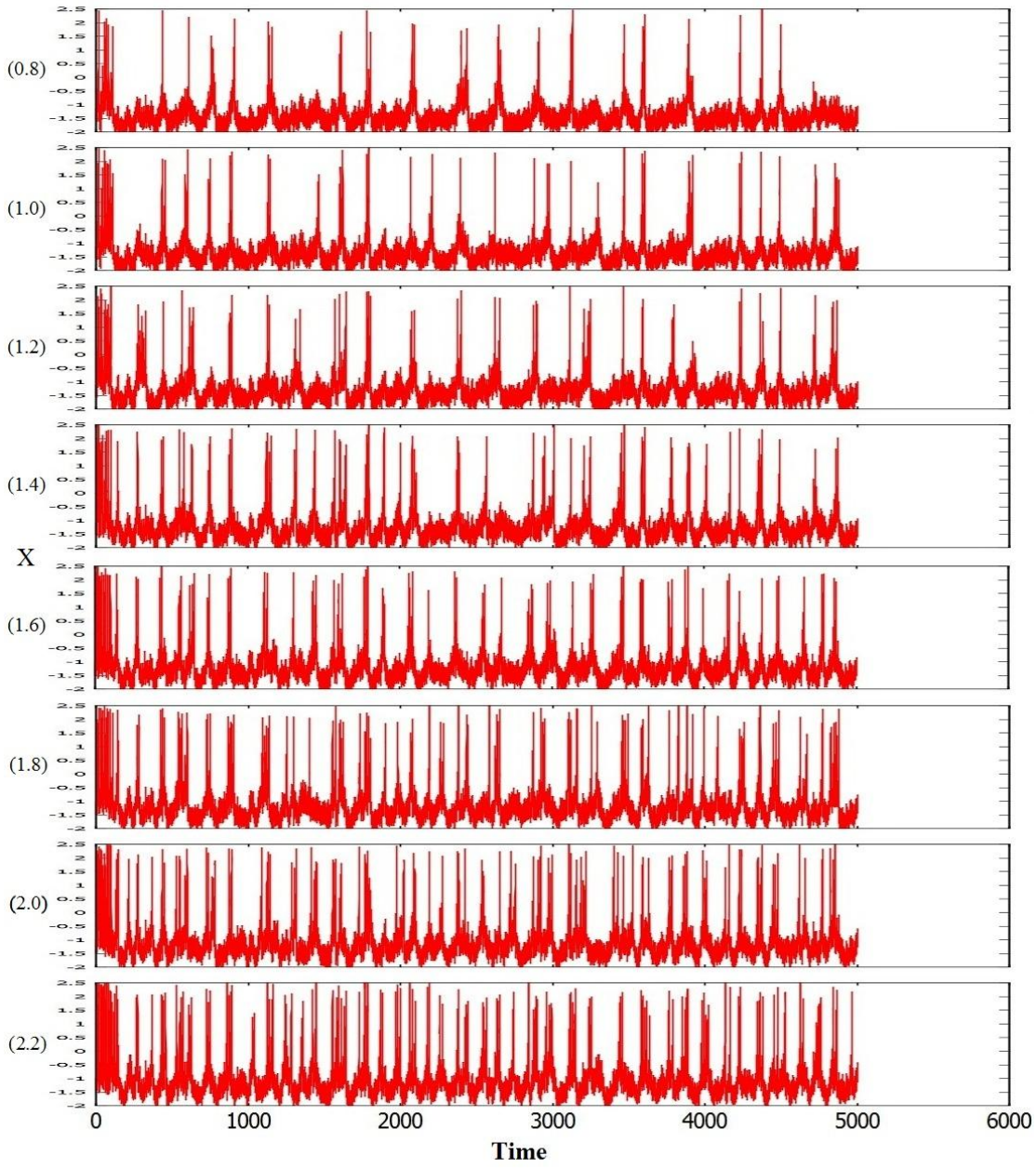

Figure 12: Voltage time series of the membrane deterministic using DSM model for the parameter values m=1, a=1, b=3, c=1, d=5, $x_s = -1.6$, *r=0.004*, *h=4*, *T=0.04* and the epsilon values are equal to zero and the noise variances is 0.8 applying various constant input current values as shown between the parentheses in the lift side of the figure.

In the figure (12) above the experiment was done by fixing the renormalization terms values to zero and the noise variance values to 0.8. And by changing the I_{base} we get the result shown in the figure above. When the value of I_{base} is changing the neuron will

start spiking from the beginning and the increase will be much better than the result gotten when the noise was zero as in figure (10). The experiments have a much better coherence compare to the result in the figure (10) but it still low.

In the figure (13) next, the result is gotten by fixing the renormalization terms values to ($\varepsilon_m^y = 0.1$,$\varepsilon_u^y = 1.0$,$\varepsilon_m^z = 0.001$ and $\varepsilon_u^z = 0.005$) and the noise variance values to 0.8 and when changing the I_{base} the number of spikes in the experiments will increase in much better and slower manner instead of the fast increasing as in the experiments done before that and the coherence will be higher in this experiments contrary to the other experiments as in figures (10, 11, 12).

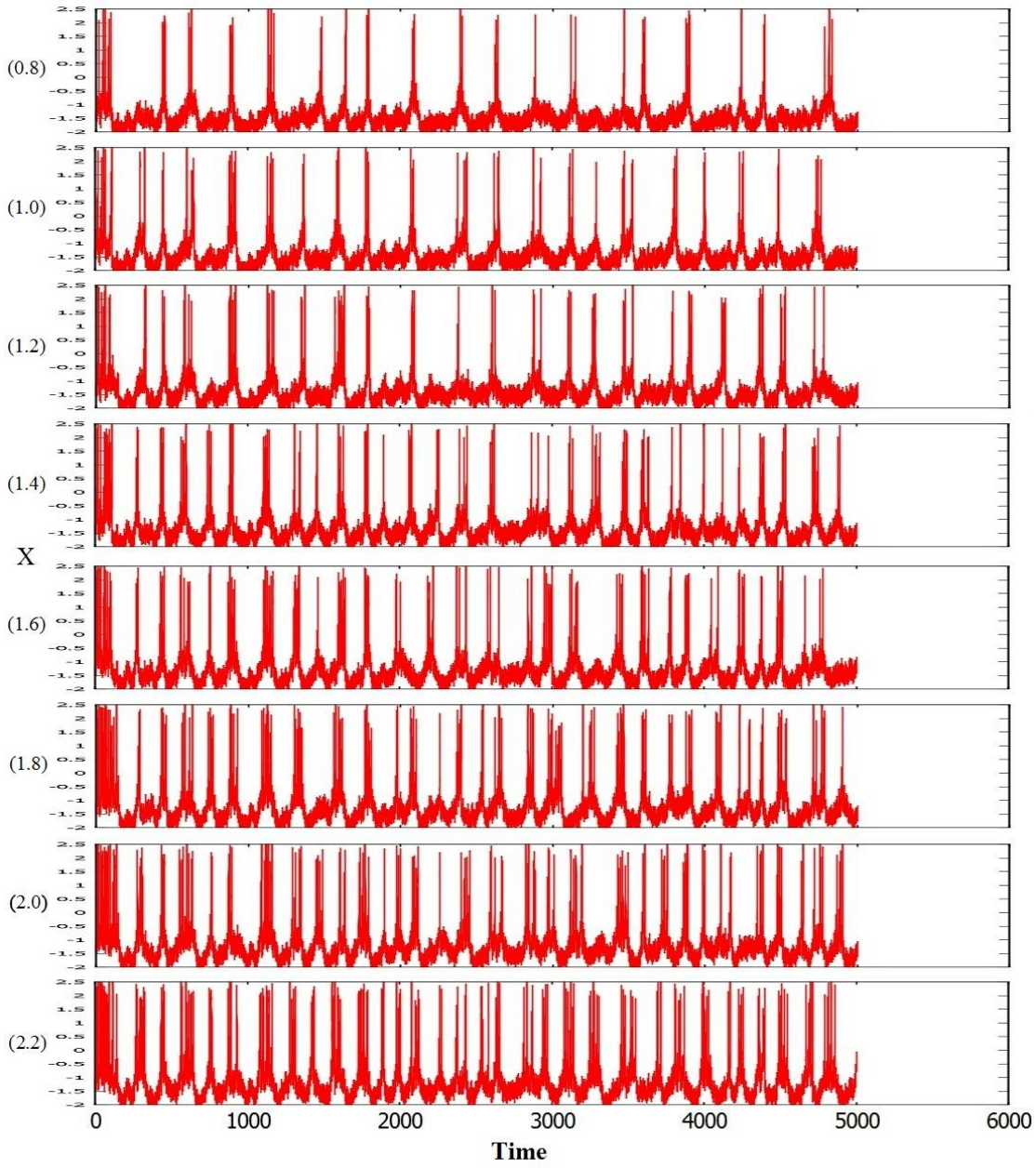

Figure 13: Voltage time series of the membrane deterministic using DSM model for the parameter values that are the same as in figure (12) and the epsilon values are as in figure (11) applying various constant input current values as shown between the parentheses in the lift side of the figure, and the noise variances is set to be equal to 0.8 in all the experiments.

In the figure (14) next, the comparison done between the results done earlier which are shown in the figures (10, 11). We got the result as shown below while using the renormalization terms in the first experiments and will take the blue color in the figure and the second experiments will take the red color in the figure and the renormalization terms are set to zero and the noise variance is set zero. The difference is very large between them.

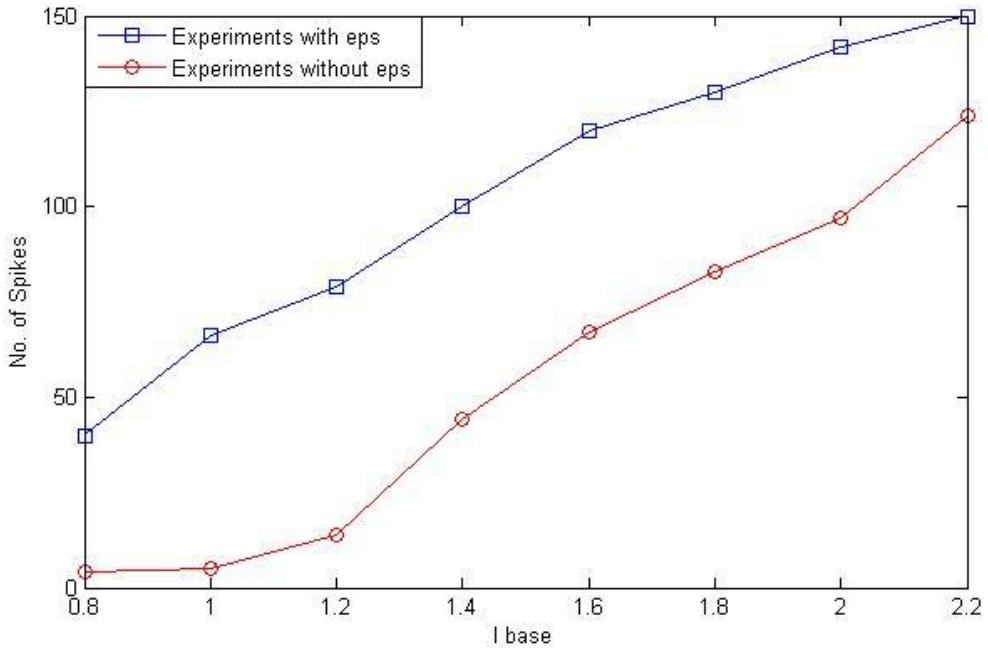

Figure 14: Shows the difference between the two experiments. In the first experiment epsilon values are set to $\varepsilon_m^y = 0.1$, $\varepsilon_u^y = 1.0$, $\varepsilon_m^z = 0.001$ and $\varepsilon_u^z = 0.005$. In the second experiment, it is set to 0. I_{base} as shown below in the figure, and the noise variances is set to zero.

In the figure (15) next, we got the result as shown below while using the renormalization terms in the first experiments and will take the blue color in the figure and the second experiments will take the red color in the figure and the renormalization terms are set to zero and the noise variance is set 0.2. The difference is smaller between them then the old comparison in figure (14).

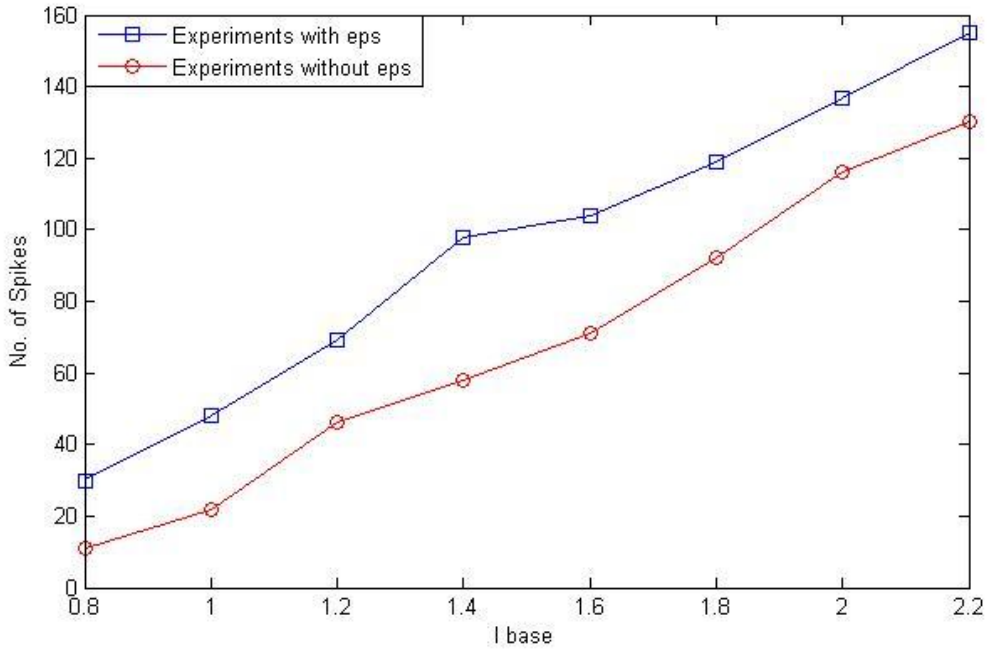

Figure 15: Shows the difference between the two experiments. In the first experiment epsilon values are set to $\varepsilon_m^y = 0.1$, $\varepsilon_u^y = 1.0$, $\varepsilon_m^z = 0.001$ and $\varepsilon_u^z = 0.005$. In the second experiment, it is set to 0. I_{base} as shown below in the figure, and the noise variances is set to (0.2).

In the figure (16) next, we got the result as shown below while using the renormalization terms in the first experiments and will take the blue color in the figure and the second experiments will take the red color in the figure and the renormalization terms are set to zero and the noise variance is set 0.5. The difference is smaller than the comparison done in figure (15).

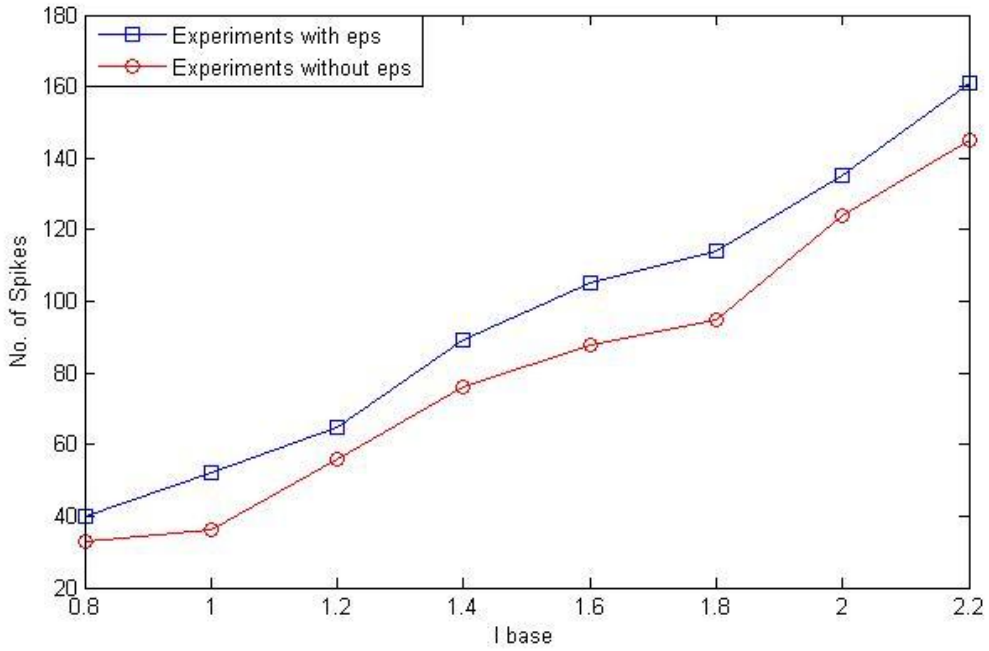

Figure 16: Shows the difference between the two experiments. In the first experiment epsilon values are set to $\varepsilon_m^y = 0.1$, $\varepsilon_u^y = 1.0$, $\varepsilon_m^z = 0.001$ and $\varepsilon_u^z = 0.005$. In the second experiment, it is set to 0. I_{base} as shown below in the figure, and the noise variances is set to (0.5).

In the figure (17) next, the comparison done between the results done earlier which are shown in the figures (12, 13). We got the result as shown below while using the renormalization terms in the first experiments and will take the blue color in the figure and the second experiments will take the red color in the figure and the renormalization terms are set to zero and the noise variance is set 0.8. The difference is very small between them compare to the other results as in figures (14, 15, 16). As the noise variance increases the difference between the existence and the absence of renormalization terms will decrease but until the last experiments it didn't vanish.

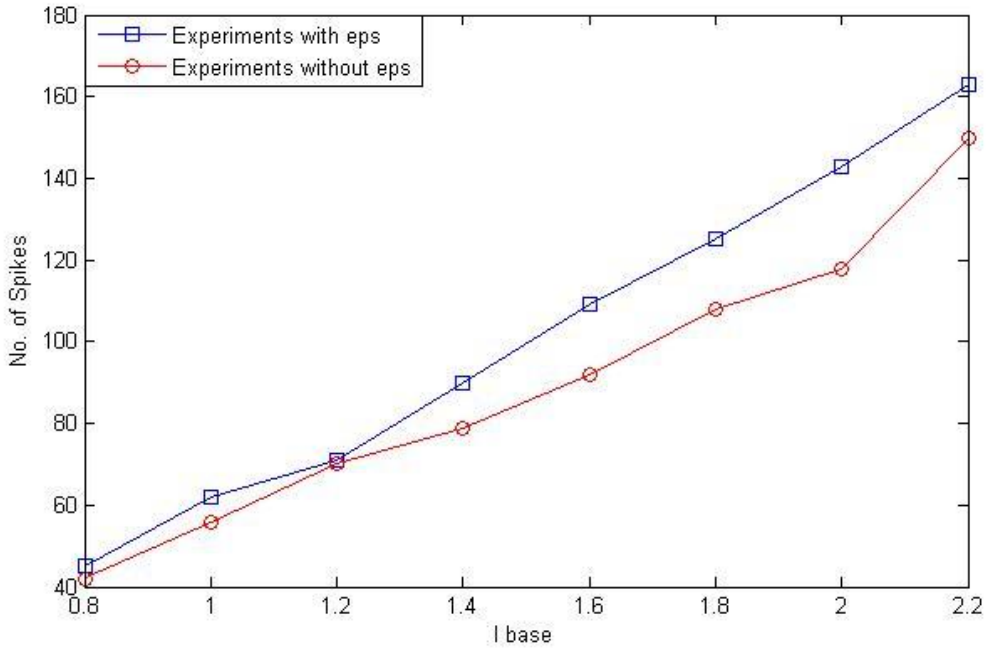

Figure 17: Shows the difference between the two experiments. In the first experiment epsilon values are set to $\varepsilon_m^y = 0.1$, $\varepsilon_u^y = 1.0$, $\varepsilon_m^z = 0.001$ and $\varepsilon_u^z = 0.005$. In the second experiment, it is set to 0. I_{base} as shown below in the figure, and the noise variances is set to (0.8).

In the next figure (18) the renormalization terms was fixed to ($\varepsilon_m^y = 0.1$, $\varepsilon_u^y = 1.0$, $\varepsilon_m^z = 0.001$ and $\varepsilon_u^z = 0.005$) and the I_{base} is fixed to 0.8 and by changing the noise variance as shown in the figure (18) below. We got the result as in the figure next.

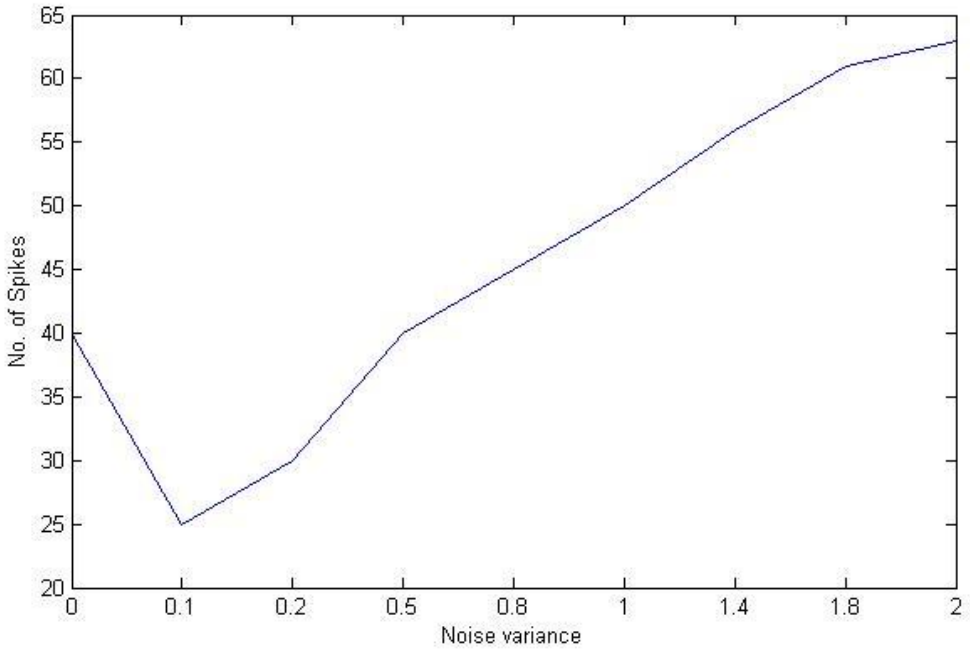

Figure 18: Shows the change in the number of spikes when the $I_{base} = 0.8$, the epsilons value are set to their default values as in figure (11) and the noise variance is changed as in the figure.

In the next figure (19) the renormalization terms was fixed to ($\varepsilon_m^y = 0.1$, $\varepsilon_u^y = 1.0$, $\varepsilon_m^z = 0.001$ and $\varepsilon_u^z = 0.005$) and the I_{base} is fixed to 1.2 and by changing the noise variance as shown in the figure (19) below. We got the result as in the figure next which shows that the renormalization terms have all the effect on the neuron around 0.5 and after the value of the noise variance pass the 0.5 limit the noise variance will have almost all the effect on the neuron and the renormalization terms effect will be much smaller.

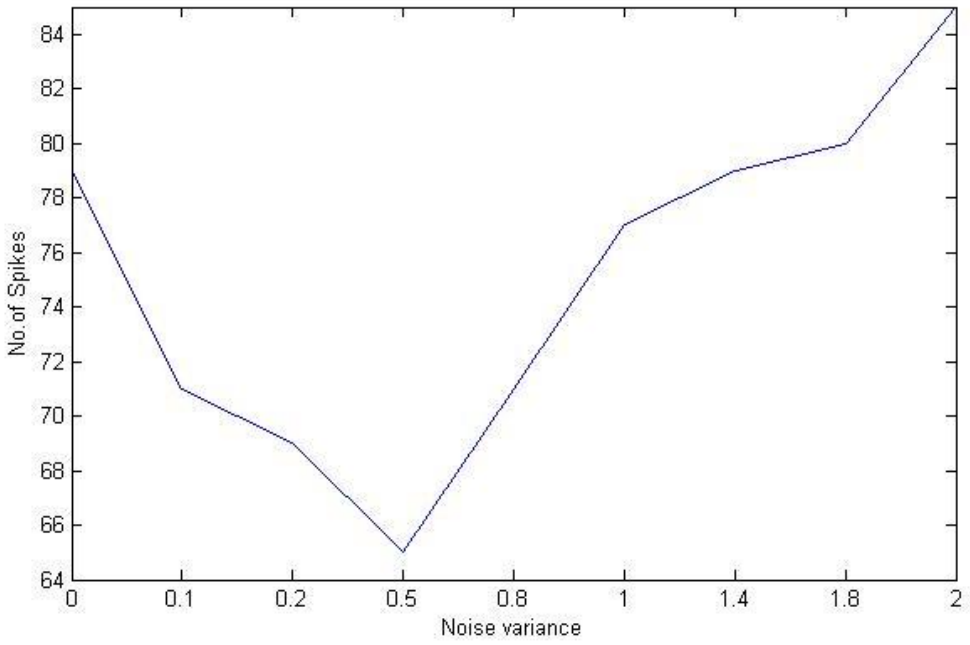

Figure 19: Shows the change in the number of spikes when the $I_{base} = 1.2$, the epsilons value is set to the default as in figure (11) and the noise variance is changed as in the figure.

In the next figure (20) the renormalization terms was fixed to ($\varepsilon_m^y = 0.1$, $\varepsilon_u^y = 1.0$, $\varepsilon_m^z = 0.001$ and $\varepsilon_u^z = 0.005$) and the I_{base} is fixed to 1.4 and by changing the noise variance as shown in the figure (20) below. We got the result as in the figure next which shows that the renormalization terms have all the effect on the neuron around 0.5 and after the value of the noise variance pass the 0.5 limit the noise variance will have almost all the effect on the neuron and the renormalization terms effect will be much smaller.

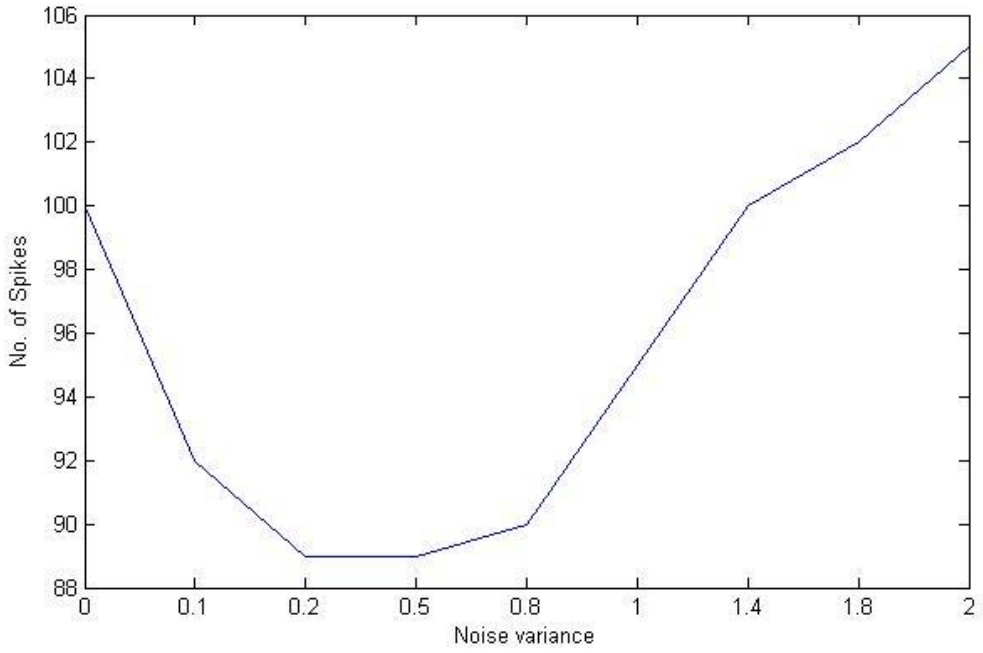

Figure 20: Shows the change in the number of spikes when the $I_{base} = 1.4$, the epsilons value is set to the default as in figure (11) and the noise variance is changed as in the figure.

In the next figure (21) the renormalization terms was fixed to ($\varepsilon_m^y = 0.1$, $\varepsilon_u^y = 1.0$, $\varepsilon_m^z = 0.001$ and $\varepsilon_u^z = 0.005$) and the I_{base} is fixed to 2.2 and by changing the noise variance as shown in the figure (21) below. We got the result as in the figure next which shows that the renormalization terms have all the effect on the neuron around 0.5 and after the value of the noise variance pass the 0.5 limit the noise variance will have almost all the effect on the neuron and the renormalization terms effect will be much smaller and as the I_{base} value increase with the noise variance the effect of the renormalization terms will be reduce in much faster manner and almost vanish.

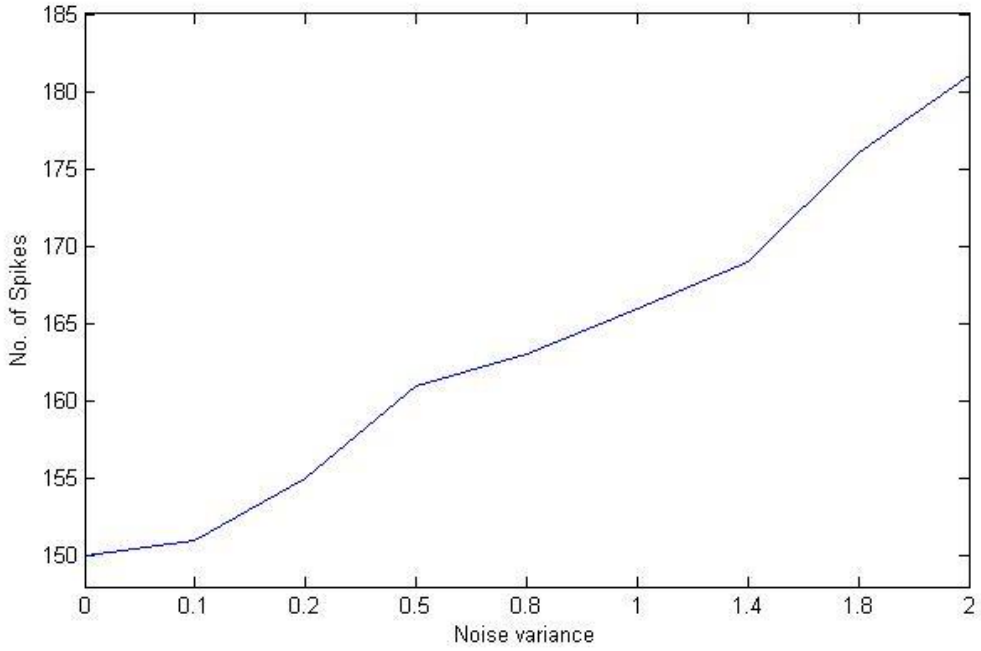

Figure 21: Shows the change in the number of spikes when the $I_{base} = 2.2$, the epsilons value is set to the default as in figure (11) and the noise variance is changed as in the figure.

Chapter 5

CONCLUSION

In this Thesis, the DSM neuron model was investigated from a numerical point of view when exposed to input current that is noisy and periodic in nature. The impacts of both the epsilon values and noise variances on the spiking rates and coherence were checked. Correction coefficients were used as an effective measure of renormalization corrections to the model. It should be considered that these renormalization corrections appear from the dilemma of being in doubt of how many open ion-channel numbers there are, even if we know the exact number of open gates.

DSM model neurons appear to be more complex than other models. It shows quicker synchronizing between two DSM neurons (Jibril and Güler 2009), dynamics of the models under constant input currents (Güler 2008) and in addition, its ability in detecting signals under noise varying and periodic input currents, that have been inspected during this study, are all the model benefits that deserve tolerating the complexity of it. Furthermore, it should be taken into consideration that this model is extremely capable of handling the small membrane sizes of the neurons.

The experiments show that the epsilon values play an important role. The absence of the epsilon values makes the neuron generate spikes at the beginning of the experiment in

slow manner and after a while the spikes generation will rise in a rapid way as shown in figures (10,12).

The existence of the epsilon values when the noise variance is under 0.5 makes the neuron spiking smother from the beginning to the end of the experiment without any large differences between any two consecutive experiments and increases the neuron spiking stability and coherence as shown in figures (11,13). The difference between the absence and existence of the epsilon values is also shown in a compared matter in the figures (14, 15).

But the figures from (18) to (21) shows that after the noise variances across the value 0.5, the effect of the epsilons values will be smaller, and the noise variances will have the most significant effects on the neuron spiking behavior and how it reacts. In addition, the noise variance almost takes all the roles played by the epsilon values from smothering the spike rates and coherence and increasing the neuron stability.

The existence of epsilon values increases the coherence in the neuron and the absence of the epsilon values reduces the coherence of the neuron. As for the noise variance using it increases the coherence of the DSM neuron model.

The results reveal that the neurons are extremely able to make a complicated and advantageous use of the channel noise in handling signals. From a technological point of view, the study shows that the DSM model has promising potential for signal detection.

5.1 Future work

As future work, we suggest an investigating in the DSM neuron model to be done on the I_{base} values between 0 and 1 while changing the renormalization terms and the noise variance or investigate the DSM neuron model under noisy input current and using various values of amplitude or frequency.

REFERENCES

Braun H.A., Huber M.T., Dewald M., Sch¨afer, K., and Voigt, K., Computer simulations of neuronal signal transduction: The role of nonlinear dynamics and noise. Int. J. Bif. Chaos 8, 881–889, 1998.

Chow C. C. and White J. A., Spontaneous action potentials due to channel fluctuations. Biophys. Journal 71: 3013-3021, 1996.

Dayan P. and Abbot L. F., Theoretical Neuroscience Computational and Mathematical Modeling of Neural Systems, MIT Press, 2002.

Faisal A. A., Selen L. P. J., and Wolpert D.M., Noise in the nervous system. Nature Revs. Neurosci. 9:292–303, 2008.

FitzHugh R. (1961) Impulses and physiological states in theoretical models of nerve membrane. Biophysical J. 1:445-466.

Fox R. F. and Y.N. Lu, Emergent collective behavior in large numbers of globally coupled independently stochastic ion channels. Phys. Rev. E, 49: 3421-3431, 1994.

Gerstner W., Kistler W., Spiking Neuron Models, Single Neurons, Populations, Plasticity, Cambridge University Press, 191, 2002.

Güler M., Modeling the effects of channel noise in neurons: A study based on dissipative stochastic mechanics. Fluct. Noise Lett. 6:L147-L159, 2006.

Güler M., Dissipative stochastic mechanics for capturing neuronal dynamics under the influence of ion channel noise. Phys. Rev. E, 76, 041918(17), 2007.

Güler M., Detailed numerical investigation of the dissipative stochastic mechanics based neuron model. J. Comput. Neurosci. 25:211–227, 2008.

Güler M., Stochastic Hodgkin-Huxley equations with colored noise terms in the conductances. Neural Computation. 25:46-74, 2013.

Hodgkin, A.L. &Huxley, A.F. (1952).A quantitative description of membrane current and its application to conduction and excitation in nerve. *Journal of Physiology (London. Print)*, *117*, 500–544.

Hindmarsh J.L. and Rose R.M., A model of neuronal bursting using three coupled first order differential equations. Proc. R. Soc. Lond. B Biol. Sci. 221, 87–102, 1984.

Jacobson G. A. et al., Sub-threshold voltage noise of rat neocortical pyramidal neurons. J. Physiology 564: 145-160, 2005.

Jibril G. O. and Güler M., The renormalization of neuronal dynamics can enhance temporal synchronization among synaptically coupled neurons. Proc. Int. Joint Conf. on Neural Networks, 1433-1438, 2009.

Kole M. H., Hallermann S., and Stuart G. J., Single Ih channels in pyramidal neuron dendrites: properties, distribution, and impact on action potential output. J. Neurosci., 26: 1677-1687, 2006.

Kolb B. and Whishaw I. Q., Fundamentals of Human Neuropsychology, Sixth Edition, Worth Publishers, 4: 83, 91, 92, 2009

Nagumo J., Arimoto S., and Yoshizawa S. (1962) An active pulse transmission line simulating nerve axon. Proc. IRE. 50:2061–2070.

Nelson E., Derivation of the Schrödinger Equation from Newtonian Mechanics, Phys. Rev. 150, 1079, 1966.

Nelson E., Dynamical Theories of Brownian Motion _Princeton University Press, Princeton, NJ, 1967.

Rose R. M. and Hindmarsh J. L., Amodel of Thalamic neuron, Proceedings of the Royal Society of London. Series B, Biological Sciences, 1984.

Sakmann B. and Neher N., Single-Channel Recording (2nd ed.) New York: Plenum 1995.

Schmid G., Goychuk I., and Hänggi P., Stochastic resonance as a collective property of ion channel assemblies. Europhys. Lett. 56: 22-28, 2001.

Schneidman E., Freedman B., and Segev I., Ion channel stochasticity may be critical in determining the reliability and precision of spike timing. Neural Comput. 10: 1679-1703, 1998.

Segev I., Cable and Compartmental Models of Dendritic Trees in Bower J. M., Beeman D., The Book of Genesis, 5: 55, 2003.

Steur E., Parameter Estimation in Hindmarsh-Rose Neurons, Traineeship report, 2006.